Eur. Phys. J. B **15**, 531–538 (2000)

THE EUROPEAN PHYSICAL JOURNAL B
EDP Sciences

Effect of electron-phonon interaction on surface states in a ternary mixed crystal

Zu Wei Yan[2,3] and Xi Xia Liang[1,2,a]

[1] CCAST (World Laboratory), PO Box 8730, Beijing 100080, P.R. China
[2] Laboratory of Solid State Physics, Department of Physics, Inner Mongolia University, Hohhot 010021, P.R. China[b]
[3] Department of Basic Sciences, Inner Mongolia Agricultural University, Hohhot 010018, P.R. China

Received 4 January 1999 and Received in final form 7 January 2000

Abstract. A variational theory is proposed to study the surface states of electrons in a semi-infinite ternary mixed crystal, by taking the effect of electron-surface optical (SO) phonon interaction into account. The energy and the wave function of the electronic surface-states are calculated. The numerical results of the energies of the surface states of the polarons and the self-trapping energies are obtained as functions of the composition x and surface potential V_0 for several ternary mixed crystal materials. The results show that the electron-phonon interaction lowers the surface-state levels with the energies from several to scores of meV. It is also found that the self-trapping energy of the surface polaron has a minimum at some middle value of the composition x. It is indicated that the electron-phonon coupling effect can not be neglected.

PACS. 63.20.Kr Phonon electron and phonon phonon interactions – 71.38.+i Polarons and electron phonon interactions – 73.20.At Surface states, band structure, electron density of states

1 Introduction

Ternary mixed crystal materials play an important role in the modern electronics. Their properties may be varied over a wide range by changing the compositions of mixed crystals. Many experimental and theoretical studies on the lattice dynamics for ternary mixed crystals have been done [1]. The random-element-isodisplacement (REI) model [2] and its modification called the modified random-element-isodisplacement (MREI) model [3,4] obtained important successes in the research on the lattice vibration of ternary mixed crystals. The electron-phonon (e-p) interaction and the intermediate coupling polaron problems in ternary mixed crystals have been studied in the framework of MREI [5–9]. A minimum for the electron – bulk longitudinal optical (LO) – phonon coupling has been found at some mediate value of the composition x in bulk ternary mixed crystals. The theoretical results qualitatively agree with the experiments [8,9]. Furthermore, the e-p interaction Hamiltonian in a slab of a ternary mixed crystal has also been obtained [5–7]. It is expected that there are two branches of surface optical (SO) phonons localized in the vicinities of the surfaces and coupling with the electrons in the ternary mixed crystal.

The electronic surface-states in polar materials have been widely studied by experimental and theoretical scientists. The rich knowledge about the surface-state energy levels, state densities and existence conditions were documented [10–13]. It is well-known that the termination of the lattice produces the intrinsic surface states, whose wave functions decay rapidly inside the material [10–12]. On the other hand, the optical phonons, in special, SO modes influence considerably the properties of electrons and sometimes introduce surface polaron states [7,14–19]. Therefore it is necessary to include e-p interactions in studying the properties of intrinsic surface states. Recently, the authors used a variational theory to study the eigenvalue problems of the surface states of polarons in binary polar crystals, including both the intrinsic surface electron states and e-p interaction effects [13,20]. The results show that the e-p coupling lowers the surface state energy. It is indicated that LO-phonon effect is unimportant when the electron is near at the surface [15,20]. However, the surface polaron problem in ternary mixed crystals is more complicated and rarely mentioned because of the presence of the multi-branches of optical phonons. Therefore a detailed investigation for this problem is necessary and the effect of electron-SO-phonon (e-SO-p) interaction should be discussed.

In the present paper, we study the effects of e-p interaction on the electronic surface states in ternary mixed crystals, by using a variational treatment in the two-band model. Both the effects of the discontinuity of lattice and the e-p interaction are considered. Since the wave functions of surface states are localized in the vicinity of

---

[a] e-mail: `xxliang@nmg2.imu.edu.cn`
[b] Mailing address

the surface [11,12], only the contribution from SO modes is involved in treating the e-p interaction as a simplified model. An effective Hamiltonian for a surface polaron in a semi-infinite ternary mixed crystal is obtained by using a Lee-Low-Pines (LLP)-like method [17,21] in Section 2. A variational calculation for the energy of surface polaronic states is performed in Section 3 and the numerical results for several practical materials are given and discussed in Section 4.

2 Surface polaron Hamiltonian

Consider a semi-infinite material system, in which the space of $z \geq 0$ is filled by ternary mixed crystal $A_xB_{1-x}C$, while the region $z < 0$ is the vacuum. An electron moves in the system and couples with lattice vibrations. Using the nearly-free-electron approximation (NFE) and our formulation for the electron-SO-phonon interaction in a slab of a ternary mixed crystal, the Hamiltonian of the electron-phonon system can be written as [6,7,12,15,17]

$$H = H_{\mathrm{e}} + H_{\mathrm{ph}} + H_{\mathrm{e-p}}, \tag{1}$$

where

$$H_{\mathrm{e}} = \frac{p_{\mathrm{t}}^2}{2m^*} + \frac{p_z^2}{2m_0} + V(z), \tag{1a}$$

$$H_{\mathrm{ph}} = \sum_{jk} \hbar\omega_{js} a_{jk}^{+} a_{jk}, \tag{1b}$$

$$H_{\mathrm{e-p}} = \sum_{jk} \left(F_{jk} \frac{\mathrm{e}^{-k|z|}}{k^{1/2}} \mathrm{e}^{\mathrm{i}\mathbf{k}\cdot\boldsymbol{\rho}} a_{jk} + \mathrm{h.c.} \right). \tag{1c}$$

In the equations, j $(= 1, 2)$ is the mode-index of SO-phonons, $\mathbf{r} = (\boldsymbol{\rho}, z)$ stands for the position vector of the electron, a_{jk}^{+} (a_{jk}) is the creation (annihilation) operator of a phonon with 2D wave-vector $\mathbf{k}$. As a traditional treatment [10–12], the parabolic band approximation is adopted to describe the motion of the electron in the x-y plane because of the displacement symmetry. The band-mass m^* of the electron in the x-y plane can be obtained by a linear interpolation

$$m^* = x m_{\mathrm{AC}} + (1-x) m_{\mathrm{BC}}, \tag{2}$$

where m_{AC} and m_{BC} are the band-masses of the electrons in the binary crystals AC and BC respectively, and m_0 is the rest mass of the electron. The 1D pseudo-potential experienced by the electron in the z-direction [11,12] is given by

$$V(z) = \begin{cases} -2V_1 \cos(2\pi z/a), & z \geq 0 \\ V_0, & z \leq 0 \end{cases} \tag{3}$$

where V_0 and V_1 are respectively the vacuum energy level and half of the forbidden band gap (FEG) E_{g} in the two-band model. Since we focus our attention on the surface-state problem and the electron is near the surface, only the SO phonon modes are taken into account in Hamiltonian (1). The coupling functions for the electron-SO-phonon interaction in (1c) are written as [6]

$$F_{js} = \left(\frac{\hbar e^2}{8\varepsilon_0 \omega_{js} A} \right)^{1/2} D_{js}, \tag{4}$$

where ω_{js} is the frequency of the jth branch of SO-modes $(j = 1, 2)$

$$\omega_{1s}^2 = \frac{2}{d_{1s}^2} \Big[\left(x\beta_1 - x^2 e_1^2 \mathit{\Gamma} \right) - 2x(1-x) e_1 e_2 C_{1s} \mathit{\Gamma} + \left((1-x)\beta_2 - (1-x)^2 e_2^2 \mathit{\Gamma} \right) C_{1s}^2 \Big], \tag{4a}$$

$$\omega_{2s}^2 = \frac{2}{d_{2s}^2} \Big[\left(x\beta_1 - x^2 e_1^2 \mathit{\Gamma} \right) C_{2s}^2 - 2x(1-x) e_1 e_2 C_{2s} \mathit{\Gamma} + \left((1-x)\beta_2 - (1-x)^2 e_2^2 \mathit{\Gamma} \right) \Big]. \tag{4b}$$

The parameter D_{js} is given by

$$D_{1s} = -\frac{6\varepsilon_0 \mathit{\Gamma}}{d_{1s}} \left[x e_1 + (1-x) e_2 C_{1s} \right], \tag{4c}$$

$$D_{2s} = -\frac{6\varepsilon_0 \mathit{\Gamma}}{d_{2s}} \left[x e_1 C_{2s} + (1-x) e_2 \right], \tag{4d}$$

with

$$d_{1s}^2 = \frac{2}{M} \big\{ x m_{\mathrm{A}} \left[(1-x) m_{\mathrm{B}} + m_{\mathrm{C}} \right] - 2x(1-x) m_{\mathrm{A}} m_{\mathrm{B}} C_{1s} + (1-x) m_{\mathrm{B}} (x m_{\mathrm{A}} + m_{\mathrm{C}}) C_{1s}^2 \big\}, \tag{4e}$$

$$d_{2s}^2 = \frac{2}{M} \big\{ x m_{\mathrm{A}} \left[(1-x) m_{\mathrm{B}} + m_{\mathrm{C}} \right] C_{2s}^2 - 2x(1-x) m_{\mathrm{A}} m_{\mathrm{B}} C_{2s} + (1-x) m_{\mathrm{B}} (x m_{\mathrm{A}} + m_{\mathrm{C}}) \big\}, \tag{4f}$$

$$\mathit{\Gamma} = -\frac{1}{6\varepsilon_0} \left\{ 1 + \left[x\alpha_1 + (1-x)\alpha_2 \right] \frac{1}{6\varepsilon_0} \right\}, \tag{4g}$$

$$\frac{\beta_1}{\mu_1} = \frac{\varepsilon_1(0) + 2}{\varepsilon_1(\infty) + 2} \omega_{T1}^2, \qquad \frac{\beta_2}{\mu_2} = \frac{\varepsilon_2(0) + 2}{\varepsilon_2(\infty) + 2} \omega_{T2}^2, \tag{4h}$$

$$\frac{\alpha_1}{V} = 3\varepsilon_0 \frac{\varepsilon_1(\infty) - 1}{\varepsilon_1(\infty) + 2}, \qquad \frac{\alpha_2}{V} = 3\varepsilon_0 \frac{\varepsilon_2(\infty) - 1}{\varepsilon_2(\infty) + 2}, \tag{4i}$$

$$\frac{e_1^2}{\mu_1 V} = 9\varepsilon_0 \frac{\varepsilon_1(0) - \varepsilon_1(\infty)}{[\varepsilon_1(\infty) + 2]^2} \omega_{T1}^2, \qquad \frac{e_2^2}{\mu_2 V} = 9\varepsilon_0 \frac{\varepsilon_2(0) - \varepsilon_2(\infty)}{[\varepsilon_2(\infty) + 2]^2} \omega_{T2}^2, \tag{4j}$$

$$C_{1s} = \frac{1}{2\mathit{\Omega}_{2s}} \left[\mathit{\Omega}_s - \left(\mathit{\Omega}_s^2 + 4\mathit{\Omega}_{1s}\mathit{\Omega}_{2s} \right)^{1/2} \right], \tag{4k}$$

$$C_{2s} = \frac{1}{2\mathit{\Omega}_{1s}} \left[-\mathit{\Omega}_s + \left(\mathit{\Omega}_s^2 + 4\mathit{\Omega}_{1s}\mathit{\Omega}_{2s} \right)^{1/2} \right], \tag{4l}$$

and

$$\begin{aligned}\Omega_s &= \frac{1}{\mu_1}\left(-x\beta_1 + x^2 e_1^2 \Gamma\right)\\ &\quad - \frac{1}{\mu_2}\left[-(1-x)\beta_2 + (1-x)^2 e_2^2 \Gamma\right],\\ \Omega_{1s} &= \frac{1}{\mu_1} x(1-x) e_1 e_2 \Gamma\\ &\quad + \frac{1}{m_{\mathrm{C}}}\left[-(1-x)\beta_2 + (1-x)^2 e_2^2 \Gamma\right],\\ \Omega_{2s} &= \frac{1}{\mu_2} x(1-x) e_1 e_2 \Gamma + \frac{1}{m_{\mathrm{C}}}\left(-x\beta_1 + x^2 e_1^2 \Gamma\right). \qquad (4\mathrm{m})\end{aligned}$$

In the above equations, M is the unit-cell mass and given by

$$M = x m_{\mathrm{A}} + (1-x) m_{\mathrm{B}} + m_{\mathrm{C}}.$$

ε_0 is the vacuum dielectric constant, $\varepsilon_l(\infty)$ and $\varepsilon_l(0)$ are respectively the high frequency and static dielectric constants, ω_{Tl} is the frequency of transverse optical (TO) phonons, β_l and e_l are the nearest-neighbor force constant and the ion effective change respectively, μ_l is the reduced mass of the two ions in a unit-cell, in the crystals "l" ($l = 1$ and 2 stands for the binary crystal AC and BC, respectively). m_{A}, m_{B} and m_{C} are the masses of the ions A, B and C, respectively.

To simplify the calculation for the effect of the electron-SO phonon interaction, we first carry out the unitary transformation

$$U_1 = \exp\left(-\mathrm{i}\sum_{jk} a_{jk}^{+} a_{jk} \mathbf{k}\cdot\boldsymbol{\rho}\right). \qquad (5)$$

Doing so, we have

$$\begin{aligned}H^* &= U_1^{-1} H U_1\\ &= \frac{1}{2m^*}\left(\mathbf{p}_t - \sum_{jk} a_{jk}^{+} a_{jk} \hbar\mathbf{k}\right)^2 + \frac{p_z^2}{2m_0} + V(z)\\ &\quad + \sum_{jk} \hbar\omega_{js} a_{jk}^{+} a_{jk} + \sum_{jk}\left[F_{js} \mathrm{e}^{-k|z|} k^{-1/2} a_{jk} + \mathrm{h.c.}\right], \qquad (6)\end{aligned}$$

where the 2D-component $\boldsymbol{\rho}$ of the electron position-vector in the x-y plane disappears and the total momentum $\mathbf{P}_t$ will be considered as a C-number.

Now let us consider a variational calculation to solve the Hamiltonian H^*. We will confine our discussion in the low-temperature limit and slow-motion electron case. Choosing an ansatz

$$|\psi\rangle = U_2 |0\rangle |\phi_\lambda(z)\rangle, \qquad (7)$$

where the wave-vector $|0\rangle$ describes the zero-phonon state of the SO-phonon field, $|\phi_\lambda(z)\rangle$ is the trial wave function with a variational parameter λ and U_2 is the unitary transformation given by

$$U_2 = \exp\left\{\sum_{jk}\left[a_{jk}^{+} f_j(\mathbf{k}) - a_{jk} f_j^*(\mathbf{k})\right]\right\}. \qquad (8)$$

The corresponding variational energy of the system being

$$E = \langle\psi| H^* |\psi\rangle = \langle\phi_\lambda(z)| H_f |\phi_\lambda(z)\rangle, \qquad (9)$$

where

$$\begin{aligned}H_f &= \langle 0| U_2^{-1} H^* U_2 |0\rangle\\ &= \frac{P_t^2}{2m^*} + \frac{p_z^2}{2m_0} + V(z) + \sum_{jk}\left[V_{jk} f_j(\mathbf{k}) + V_{jk}^* f_{jk}^*(\mathbf{k})\right]\\ &\quad + \frac{\hbar^2}{2m^*}\left[\sum_{jk} \mathbf{k}\,|f_j(\mathbf{k})|^2\right]^2\\ &\quad + \sum_{jk}\left[\hbar\omega_{js} - \frac{\hbar\mathbf{k}\cdot\mathbf{P}_t}{m^*} + \frac{\hbar^2 k^2}{2m^*}\right]|f_j(\mathbf{k})|^2 \qquad (10)\end{aligned}$$

with

$$V_{jk} = F_{js}\frac{\mathrm{e}^{-k|z|}}{k^{1/2}}\,. \qquad (11)$$

The displacement amplitude $f_j(\mathbf{k})$ and its conjugate $f_j^*(\mathbf{k})$ are determined by minimizing H_f [17,21] as follows

$$\frac{\partial H_f}{\partial f_j(\mathbf{k})} = \frac{\partial H_f}{\partial f_j^*(\mathbf{k})} = 0, \qquad (12)$$

which gives

$$f_j^*(\mathbf{k}) = \frac{-V_{jk}}{\left[\hbar\omega_{jk} - \frac{\hbar\mathbf{k}\cdot\mathbf{P}_t(1-\eta)}{m^*} + \frac{\hbar^2 k^2}{2m^*}\right]}, \qquad (13\mathrm{a})$$

with

$$\frac{\eta}{1-\eta} = \sum_j \alpha_{js}\gamma_j(z), \qquad (13\mathrm{b})$$

where

$$\alpha_{js} = \frac{e^2}{8\pi\varepsilon_0^2\hbar\omega_{js}}\left(\frac{m^*}{2\hbar\omega_{js}}\right)^{1/2} D_{js}^2, \qquad (13\mathrm{c})$$

is the coupling constant between the electron and the jth branch of SO-phonons,

$$\gamma_j(z) = \int_0^\infty \frac{2u_{js}^3 \mathrm{e}^{-2k|z|} k^2 \mathrm{d}k}{\left(k^2 + u_{js}^2\right)^3}, \qquad (13\mathrm{d})$$

and u_{js} is defined by

$$u_{js} = \left(\frac{2m^*\omega_{js}}{\hbar}\right)^{1/2}. \qquad (14)$$

Inserting (13) into (10) leads to

$$H_f = \sum_j \frac{P_t^2}{2m^* \left[1 + \alpha_{js}\gamma_j(z)\right]} + \frac{p_z^2}{2m_0} + V(z) + V_{\text{eff}}(z), \tag{15}$$

where V_{eff} is a 1D effective potential

$$V_{\text{eff}} = -\sum_j \alpha_{js}\hbar\omega_{js}\beta_j(z) \tag{16}$$

and

$$\beta_j(z) = \int\limits_0^\infty \frac{u_{js}\mathrm{e}^{-2k|z|}\mathrm{d}k}{k^2 + u_{js}^2}\cdot \tag{17}$$

Here H_f includes the contribution of the e-p interaction and is called the effective polaron Hamiltonian.

Since we are concerned with only the surface state and the electron transverse motion is unimportant, we can set $P_t = 0$ without loss of generality in the following. Therefore the effective polaron Hamiltonian can be simplified to be

$$H_{\text{eff}} = \frac{p_z^2}{2m_0} + V(z) + V_{\text{eff}}(z). \tag{18}$$

3 Variational energy

We now start with the effective Hamiltonian (18) to calculate the surface-state energy of the polaron. The corresponding variational energy is given by

$$E_v = \langle \phi_\lambda(z)|\, H_{\text{eff}}\, |\phi_\lambda(z)\rangle\,. \tag{19}$$

Here the trial wave-function $|\phi_\lambda(z)\rangle$ can be well-chosen to be similar to the nearly-free-electron approximation (NFEA) wave-function of intrinsic surface states [12,13].

A NFEA perturbation theory (NFEPT) has been used to seek the solutions for a Hamiltonian in a binary crystal without including the e-p interaction [10,12], where the surface-state eigenfunction was found to be

$$|\psi\rangle = \begin{cases} A\mathrm{e}^{-\mu z}\cos(\pi z/a + \delta), & z \geq 0 \\ B\mathrm{e}^{q_0 z}, & z \leq 0 \end{cases} \tag{20}$$

where the energy E and parameters q_0, μ and δ were determined by some equations [12]. However, the NFEPT method becomes invalid when the band gap is so broad that the perturbation can not be treated as a small disturbance. A variational method has been used to improve the result [13,20], which works well in a larger range of the band gap. The trial wave function is then chosen as

$$|\phi_\lambda(z)\rangle = \begin{cases} A\mathrm{e}^{-\lambda_1 z}\cos(\pi z/a + \lambda_2), & z \geq 0 \\ B\mathrm{e}^{qz} & z \leq 0 \end{cases} \tag{21a}$$

where λ_1 and λ_2 are treated as variational parameters. Matching $\phi_\lambda(z)$ and $\phi'_\lambda(z)/\phi_\lambda(z)$ at $z = 0$, provides the relationships:

$$A\cos\lambda_2 = B, \tag{21b}$$

$$q = -\left(\lambda_1 + \frac{\pi}{a}\tan\lambda_2\right), \tag{21c}$$

while A is determined by

$$A^{-2} = -\frac{\cos^2\lambda_2}{2\left(\lambda_1 + \dfrac{\pi}{a}\tan\lambda_2\right)} + \frac{1}{4}\left(\frac{\lambda_1\cos 2\lambda_2 - \dfrac{\pi}{a}\sin 2\lambda_2}{\lambda_1^2 + \pi^2/a^2} + \frac{1}{\lambda_1}\right)\cdot \tag{22}$$

Inserting (21) into (19), the expectation value of H_{eff} is given by

$$E_v = \frac{\pi^2\hbar^2A^2}{8m_0a^2\lambda_1} - \frac{V_0}{2}\,\frac{A^2\cos\lambda_2}{\lambda_1 + \dfrac{\pi}{a}\tan\lambda_2} - \frac{V_1A^2}{4}\left(\frac{\cos 2\lambda_2}{\lambda_1} + \frac{2\lambda_1}{\lambda_1^2 + \pi^2/a^2} + \frac{\lambda_1\cos 2\lambda_2 - \dfrac{2\pi}{a}\sin 2\lambda_2}{\lambda_1^2 + 4\pi^2/a^2}\right) - \sum_j E_{e-js}, \tag{23}$$

where

$$E_{e-js} = \alpha_{js}\hbar\omega_{js}A^2\left(I_j + g_j\cos^2\lambda_2\right), \tag{24}$$

with

$$I_j = \int\limits_0^\infty \frac{u_{js}}{4\left(k^2 + u_{js}^2\right)} \times \left(\frac{1}{\lambda_1 + k} + \frac{(\lambda_1 + k)\cos 2\lambda_2 - \dfrac{\pi}{a}\sin 2\lambda_2}{(\lambda_1 + k)^2 + \pi^2/a^2}\right)\mathrm{d}k, \tag{25a}$$

and

$$g_j = -\int\limits_0^\infty \frac{u_{js}\mathrm{d}k}{2\left(k^2 + u_{js}^2\right)\left(\lambda_1 + \dfrac{\pi}{a}\tan\lambda_2 - k\right)}\cdot \tag{25b}$$

The variational parameters are determined by the following equation

$$\frac{\partial E_v}{\partial \lambda_i} = 0, \qquad i = 1, 2. \tag{26}$$

Solving numerically the equation (26) for practical materials, one can obtain the minimum of the variational energy E_v as the surface-state energy E_s.

The last term in (23) can be written as

$$E_{\text{tr}} = \sum_j E_{e-js} = E_{\text{tr}1} + E_{\text{tr}2} = E_{e-1s} + E_{e-2s}, \tag{27}$$

Table 1. Parameters of some III–V and II–VI components. Energy is measured in meV and mass in electron rest mass m_0.

Materials	ε_0	ε_∞	$m(m_0)$	$\hbar\omega_{TO}$	$\hbar\omega_{LO}$
AlAs[a]	10.06	8.16	0.150	44.8	50.09
GaAs[a]	13.18	10.89	0.067	33.29	36.25
GaP[b]	10.28	8.46	0.338	45.31	49.96
InP[b]	12.29	9.56	0.076	38.20	43.32
ZnSe[b]	8.33	5.90	0.171	25.67	30.50
ZnTe[b]	9.86	7.28	0.160	21.95	25.42

[a] Reference [22]. [b] Reference [23].

Table 2. Lattice constants and E_g used in the computations for several ternary mixed crystals. Energy is measured in meV.

Material	a (Å)	E_g
$Al_xGa_{1-x}As$[c]	$5.6533 + 0.0078x$	$1425 + 1155x + 370x^2$
$Ga_xIn_{1-x}P$[d]	$5.8696 - 0.418x$	$1350 + 668x + 758x^2$
$ZnSe_xTe_{1-x}$[e]	$6.1037 - 0.435x$	$2390 + 433x$

[c] Reference [22]. [d] Reference [24]. [e] Linear interpolation.

and called as the self-trapping energy of the surface polaron. Here the terms of $j = 1$ and 2 correspond to the contributions of the electron-phonon interactions from two different branches of SO-phonons, respectively. It is seen from (23) and (27) that the electron-SO-phonon coupling lowers the energy of the surface-state polaron with the value of the self-trapping energy E_{tr}.

4 Numerical results and discussion

We have numerically computed the surface-state energies of the polaron for several ternary mixed crystal materials. For the sake of comparison we have also calculated the surface state energies of the electron without including the e-p interactions. As examples we illustrate the numerical results for the ternary mixed crystals $Al_xGa_{1-x}As$, $Ga_xIn_{1-x}P$ and $ZnSe_xTe_{1-x}$ in Figures 1–4. The parameters used in the computations are listed respectively in Table 1 and Table 2 for binary and ternary mixed crystals.

Figure 1 shows the surface-state energy levels as functions of the compositions x for the ternary mixed crystal materials listed in Table 2, here we put the surface potential to be a reasonable value $V_0 = 5.0$ eV in the computations for reference. For comparison, both the curves of the energy levels including (E_s^p) and ignoring (E_s^0) the e-p interactions are also plotted in the same figure. It is clearly seen from Figure 1 that the surface-state levels as functions of the composition x are monotonous for $ZnSe_xTe_{1-x}$ and non-monotonous for $Al_xGa_{1-x}As$ and $Ga_xIn_{1-x}P$, corresponding to the linear and square variations of the width E_g of the FEG with increasing the composition x.

As is expected that the surface-states including the e-p interaction are always lower than that without including the phonon effects for all the computed materi-

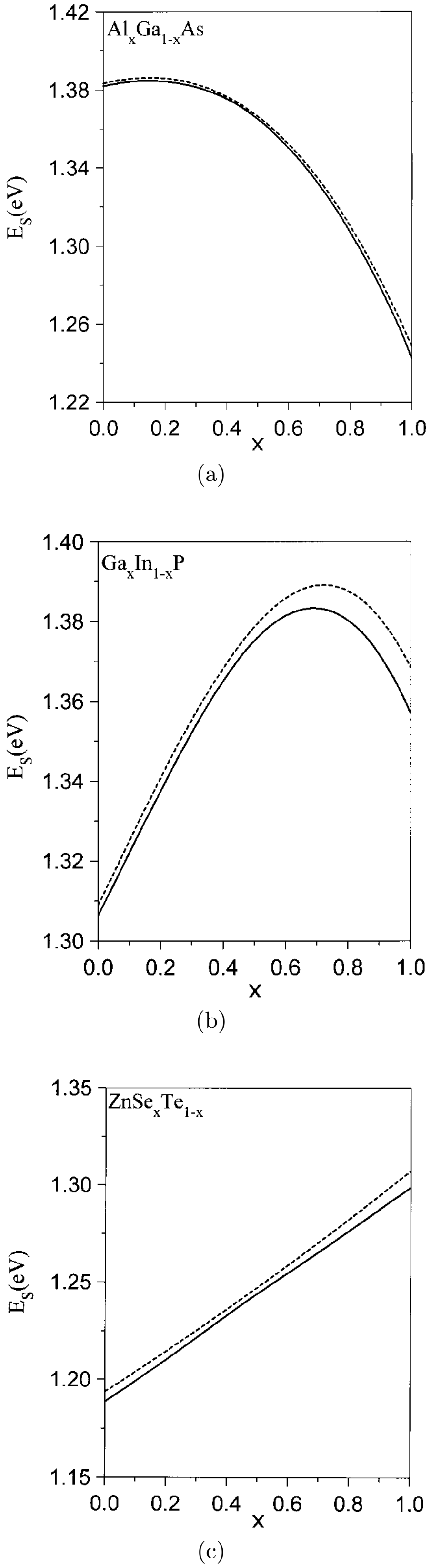

Fig. 1. Surface-states energies E_S with (solid lines) and without (dashed lines) electron-phonon interactions as functions of composition x for ternary mixed crystals: (a) $Al_xGa_{1-x}As$, (b) $Ga_xIn_{1-x}P$ and (c) $ZnSe_xTe_{1-x}$.

Table 3. FEG, ΔE_{ph} for some ternary mixed crystals. Energy is measured in meV.

Material	$x = 0.2$		$x = 0.8$	
	E_{g}	ΔE_{ph}	E_{g}	ΔE_{ph}
$\mathrm{Al}_x\mathrm{Ga}_{1-x}\mathrm{As}$	1671	−1.58	2586	−3.14
$\mathrm{Ga}_x\mathrm{In}_{1-x}\mathrm{P}$	1514	−3.27	2370	−7.34
$\mathrm{ZnSe}_x\mathrm{Te}_{1-x}$	2479	−4.34	2736	−6.03

als. In other words, the e-p interaction lowers the energy levels of the surface states. It is also found in Figure 1 that the two curves of the surface-state levels with and without the phonon effects are separated by a few meV (around 1 ~ 10 meV). The curves in Figure 1a almost coincident for the weak e-p coupling ternary mixed crystal $\mathrm{Al}_x\mathrm{Ga}_{1-x}\mathrm{As}$. However, the curves for the materials $\mathrm{Ga}_x\mathrm{In}_{1-x}\mathrm{P}$ and $\mathrm{ZnSe}_x\mathrm{Te}_{1-x}$ in Figure 1b and Figure 1c are separated distinctly from each other. On the other hand, the surface-state shifts are also related to the width of FEG. Table 3 lists the FEG widths E_{g} and the energy shifts $\Delta E_{\mathrm{ph}} = E_s^p - E_s^0$ of surface-states by the e-p interaction for the above materials with $x = 0.2$ and $x = 0.8$, respectively. It can be seen that the broader FEG generally causes the greater shift for the surface state level. The phonon effects are smaller for weak e-p coupling or narrow band gap materials, such as $\mathrm{Al}_{0.2}\mathrm{Ga}_{0.8}\mathrm{As}$ and $\mathrm{Ga}_{0.2}\mathrm{In}_{0.8}\mathrm{P}$ (around 1.5 ~ 3.0 meV), but are considerable for the others, such as $\mathrm{Ga}_{0.8}\mathrm{In}_{0.2}\mathrm{P}$ and $\mathrm{ZnSe}_{0.8}\mathrm{Te}_{0.2}$ (around 6 ~ 8 meV) with stronger e-p coupling or broad band gaps. It follows that the stronger the e-p coupling or broader width is, the greater the shift of surface state.

We have also computed the surface-state energy levels as functions of the surface potential V_0, which has been chosen to vary in the reasonable range 3.9–5.7 eV [12] in the computations. The results of E_s^p and E_s^0 for the materials listed in Table 2 are shown as functions of the surface potential V_0 in Figure 2. It is seen that the surface state shifts by SO-phonons are almost independent of V_0. It will be seen from this that choosing the surface potential as $V_0 = 5.0$ eV does not loss the generality.

To clear understand the feature of the e-SO-p interaction effects in the ternary mixed crystal, we have plotted the e-SO-p coupling constants α_{s1} and α_{s2} as functions of the composition x in Figure 3, where the surface potential V_0 is chosen as a typical value 5.0 eV. It is shown that the feature of coupling between electron with two branch SO-phonon is obvious different. The coupling constant α_{s1} is larger than α_{s2} in the whole range of the composition x, and the value of α_{s1} (α_{s2}) gets the value corresponding to that in the end material AC (BC) at $x = 0$ and $x = 1$. Therefore the characteristics for the coupling constants α_{s1} and α_{s2} can be recognized as two-mode behavior [2–4,9]. It is also found that the dependence of α_{s1} on the composition x is nearly linear, but α_{s2} intensely changes and has a minimum at a mediate value of x.

In Figure 4, we have illustrated the shifts of the surface-state by SO-phonons as functions of x with $V_0 = 5.0$ eV. It is clearly seen that the self-trapping energy of

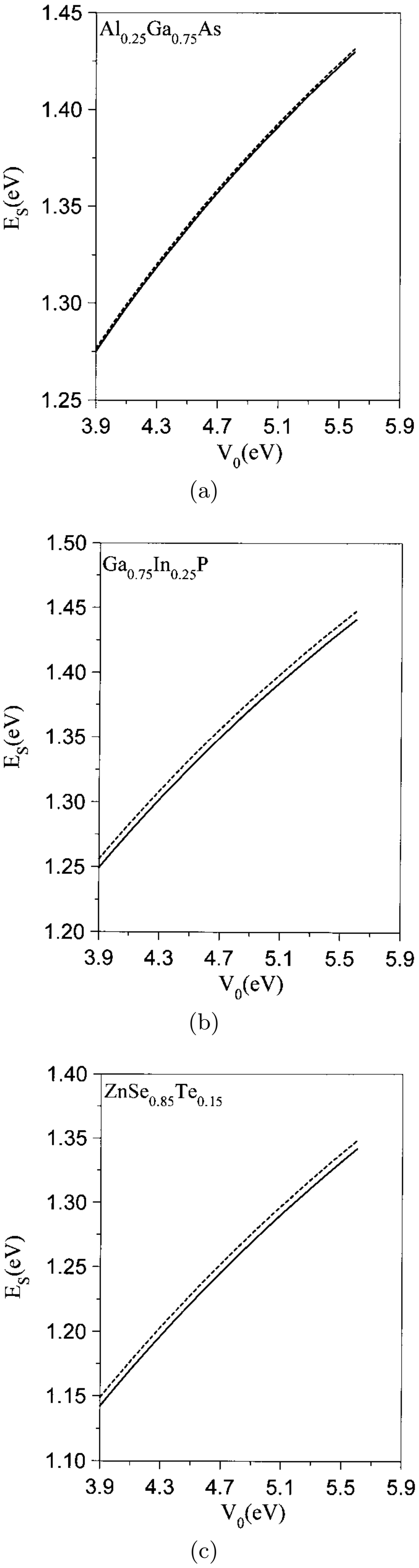

Fig. 2. The surface-states energies E_{S} with (solid lines) and without (dashed lines) electron-phonon interactionsas functions of the surface potential barrier V_0 for ternary mixed crystals: (a) $\mathrm{Al}_{0.25}\mathrm{Ga}_{0.75}\mathrm{As}$, (b) $\mathrm{Ga}_{0.75}\mathrm{In}_{0.25}\mathrm{P}$ and (c) $\mathrm{ZnSe}_{0.85}\mathrm{Te}_{0.15}$.

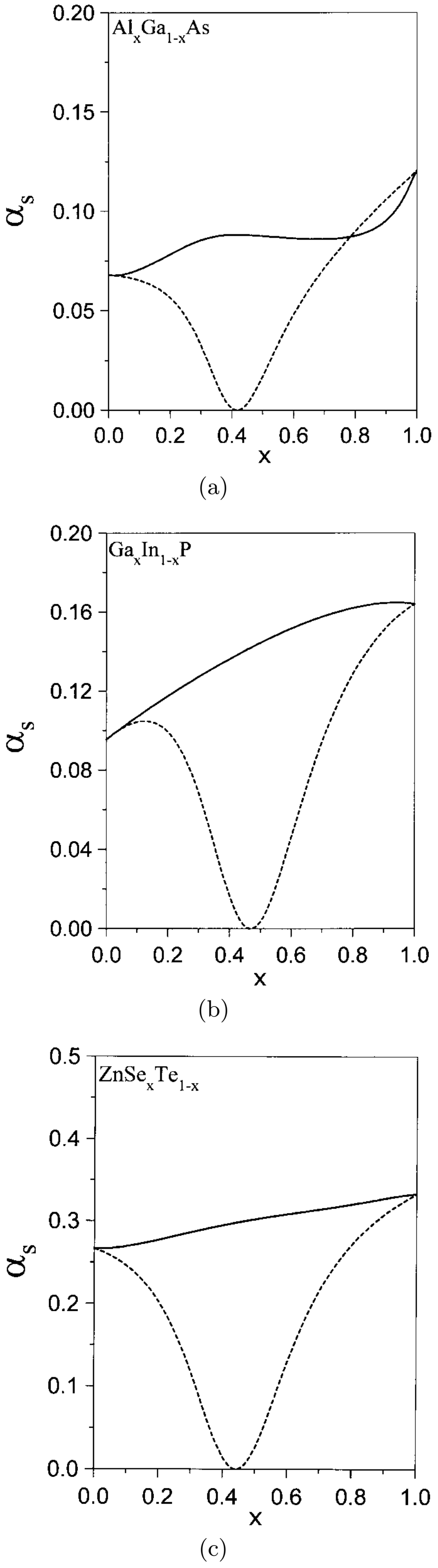

(a)

(b)

(c)

Fig. 3. Electron-SO-phonon coupling constants α_{s1} (solid line) and α_{s2} (dashed line) as functions of the composition x for ternary mixed crystals: (a) $Al_xGa_{1-x}As$, (b) $Ga_xIn_{1-x}P$ and (c) $ZnSe_xTe_{1-x}$.

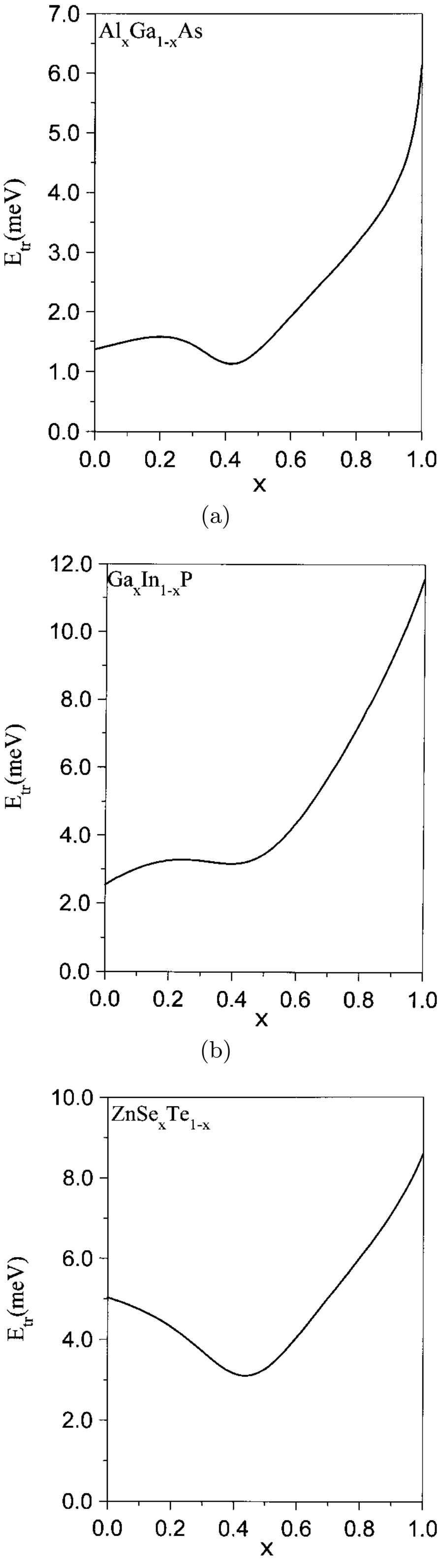

(a)

(b)

(c)

Fig. 4. The self-trapping energy $E_{\rm tr}$ as function of the composition x for ternary mixed crystals: (a) $Al_xGa_{1-x}As$, (b) $Ga_xIn_{1-x}P$ and (c) $ZnSe_xTe_{1-x}$.

the surface polarons as function of x is non-monotonous and has a local minimum at a middle value between $x = 0.4$ and $x = 0.5$ for all the materials we computed. The analogous feature was also found for bulk materials of ternary mixed crystals [8,9]. The minimum of e-p coupling can be explained as that the two polarization-waves due to respectively the A-C and B-C ion-pairs disturb by each other.

At the end of $x = 0$, the ternary mixed crystal reduces to the binary crystal BC. With increasing the composition x, the impurities of A-ions are doped into the system, so that the propagation of the BC-like polarization-wave is turned into difficult and the corresponding e-p coupling decays. In the meanwhile, AC-like phonon modes are almost localized and contribute nothing to the e-p coupling. At the other end, *i.e.* $x = 1$, a similar situation is shown for AC-like polarization-wave. Therefore the total e-p coupling decreases with x and gets their minimum at the near middle value of composition x.

Nevertheless, the characteristics of the curves for surface states are dramatically different from that of bulk polarons [9]. The e-p contributions to the surface-states come from two SO-phonon branches, whose frequencies and the e-p coupling behavior are different from that in bulk [2,3,9]. In addition, the dependence of the width of FEG on the composition x in the way of monotonous or non-monotonous also causes different e-p coupling contributions (see Tab. 3). The varied factors make the complexity of the curves for surface polarons.

Moreover, it is also found that the strengths of the phonon effects for varied systems are obviously different. The self-trapping energies are smaller for the weaker e-p coupling and narrower forbidden zone materials, such as $\mathrm{Al_{0.2}Ga_{0.8}As}$ and $\mathrm{Ga_{0.2}In_{0.8}P}$ materials, but larger for the materials with stronger e-p coupling and wider FEG, such as $\mathrm{Ga_{0.8}In_{0.2}P}$ and $\mathrm{ZnSe_{0.8}Te_{0.2}}$ materials.

In summary, we have investigated the surface states of an electron in a semi-infinite ternary mixed crystal including e-SO-p interaction by a variational treatment. The energy level of a surface polaron state has been calculated. The effects of the e-SO-p interaction on the surface states are obtained for some ternary mixed crystal materials. The numerical results show that the e-p coupling lowers the surface-state levels from several to scores of meV. Therefore the phonon effects can not be neglected, especially for materials with stronger e-p couplings and broad band gaps. As a striking character, a minimum of the contribution of the electron-phonon interaction to the energy of the surface polaron in a ternary mixed crystal is also found.

The work was supported by the National Natural Science Foundation of China (Project 19764001) and the Natural Science Foundation of Inner Mongolia Autonomous Region of China.

References

1. D.W. Taylor, in *Optical properties of mixed crystals*, edited by R.J. Elliott, I.P. Ipatovd (North-Holland, Amsterdam, 1988), Chap. 2.
2. Y.S. Chen, S.S. Shockly, G.L. Reaeson, Phys. Rev. **151**, 648 (1966).
3. I.F. Chang, S.S. Mitra, Adv. Phys. **20**, 359 (1971).
4. L. Genzel, T.P. Martin, C.H. Perry, Phys. Status Solidi B **62**, 83 (1974).
5. G. Verbist, F.M. Peeters, J.T. Devreese, Ferroelectrics **130**, 27 (1992).
6. X. Wang, X.X. Liang, Phys. Rev. B **42**, 8915 (1990); Acta Scientiarum Naturelium Universitatis Intramongolicae **23**, 80 (1992).
7. G.Q. Hai, F.M. Peeters, J.T. Devreese, Phys. Rev. B **48**, 4666 (1993).
8. S. Mimotogi, T. Masumi, J. Phys. Soc. Jpn **61**, 1701 (1992).
9. X.X. Liang, Y.S. Zhang, Z. Phys. B **91**, 455 (1993).
10. S.G. Davison, J.D. Levine, in *Solid State Physics*, edited by H. Ehrenreich, F. Seitz, D. Turnbull (Academic Press, New York, 1970), Vol. 25.
11. F. Garcia-Moliner, F. Flores, J. Phys. C **9**, 1609 (1976).
12. S.G. Davison, M. Steslicka, *Basic Theory of Surface States* (Clarendon Press, Oxford, 1992), Chap. 5.
13. X.X. Liang, Z.W. Yan, Surf. Sci. **400**, 232 (1998).
14. J. Sak, Phys. Rev. B **6**, 3981 (1972).
15. E. Evans, D.L. Mills, Phys. Rev. B **8**, 4004 (1973).
16. N. Mori, T. Ando, Phys. Rev. B **40**, 6175 (1989).
17. X.X. Liang, S.W. Gu, Solid State Commun. **50**, 505 (1984).
18. Y.J. Wang, H.A. Nickel, B.D. McCombe, F.M. Peeters, J.M. Shi, G.Q. Hai, X.-G. Wu, Phys. Rev. Lett. **79**, 3226 (1997).
19. Wu. Xiaoguang, F.M. Peeters, J.T. Devreese, Phys. Rev. B **40**, 4090 (1989).
20. Z.W. Yan, X.X. Liang, Solid State Commun. **110**, 451 (1999).
21. T.D. Lee, F.E. Low, D. Pines, Phys. Rev. **90**, 297 (1953).
22. S. Adachi, J. Appl. Phys. **58**, R1 (1985).
23. E. Kartheuser, in *Polarons in Ionic Crystals and Polar Semiconductors* (North-Holland Amsterdam, 1972), p. 718.
24. R.E. Nahory, M.A. Pollack, W.D. Johnston, Appl. Phys. Lett. **33**, 659 (1978).